

SELF-CLEANING COATINGS FOR SAND STONES

¹Kryštof FONIOK, ²Blanka KOLINKEOVÁ, ²Jiří ŠČUČKA, ¹Vlastimil MATĚJKA

¹VSB - Technical University of Ostrava, Faculty of Materials Science and Technology, Ostrava, Czech Republic, EU, krystof.foniok@vsb.cz, vlastimil.matejka@vsb.cz

²Institute of Geonics, Czech Academy of Sciences, Ostrava, Czech Republic, EU, blanka.kolinkeova@ugn.cas.cz, jiri.scucka@ugn.cas.cz

<https://doi.org/10.37904/nanocon.2024.5015>

Abstract

In this research, we tested the performance of the self-cleaning coatings based on exfoliated g-C₃N₄ applied on the surface of sandstone. Research activities include: i) preparation of exfoliated g-C₃N₄, ii) preparation of exfoliated g-C₃N₄ water suspensions, iii) application of the suspensions on the surface of the sandstone samples, and iv) testing of the self-cleaning performance. Exfoliated g-C₃N₄ was prepared by thermal exfoliation of bulk g-C₃N₄ prepared by thermal polycondensation of melamine. Samples were characterized using elemental analysis, infrared spectroscopy, scanning electron microscopy, the band gap values were determined with help of reflectance spectra measured using UV-VIS DRS spectrometry. Rhodamine B dye was used a model substance to evaluate the photodegradation activity of prepared samples, and the results showed significantly better photodegradation performance of exfoliated sample, which was further used for application on the surface of sand stone. Water suspensions of g-C₃N₄ (2 and 4 g·dm⁻³) were prepared and applied on the surface of the sandstone samples using the spraying technique. Such prepared samples were subjected to the self-cleaning performance test based on the discoloration of rhodamine B under VIS irradiation and constant humidity and temperature. Changes in the a* coordinate in CIE L*a*b* color space were used to quantitatively monitor the discoloration of the tested samples.

Keywords: Graphitic carbon nitride, sand stones, photocatalysis, self-cleaning surfaces

1. INTRODUCTION

Photodegradation of environmental pollutants over photocatalytically active materials, for example, TiO₂, ZnO, and recently g-C₃N₄, has been widely studied topic for many years, and many scientific articles have been published on the use of photodegradation processes in the fields of water purification. Comprehensive reviews of these applications are summarized, for example, in the following papers [1, 2]. However, interest in research on the application of heterogeneous photocatalysis in the building industry has been noted relatively recently. The creation of photocatalytically active surfaces on the walls of buildings represents a promising way of cleaning the surrounding atmosphere, eliminating the growing of algae on the surfaces, and assuring the self-cleaning properties of the surfaces with deposited photocatalysts [3, 4]. As examples of the application of photocatalytically active TiO₂ in the building industry is the jubilee church Dives in Misericordia in Rome opened in 2003, the Hospital Manuel Gea Gonzalez in Mexico City opened in 2013 [5].

So far, the most commonly used photocatalytically active material used in building industry is titanium dioxide (TiO₂). In general, TiO₂ is considered as one of the most effective photocatalysts due to its strong oxidative ability and long-term photostability. The common crystallographic phases of TiO₂ are anatase, rutile and brookite, whereas the anatase is the TiO₂ phase showing higher photodegradation activity. Anatase is the semiconductor with large bandgap at around 3.2 eV [6]. This energy value determines that the wavelength 388 nm and lower is necessary to evoke the photocatalytic activity of anatase, and the radiation of this

wavelength belongs to UV region. The day light contains around 5% of the light available for anatase activation, and thus alternatives to TiO_2 with lower band gap values are intensively searched.

Graphitic carbon nitride ($\text{g-C}_3\text{N}_4$) has attracted a great interest after Wang et al. [7] discovered its ability of photocatalytic water splitting. The band gap of $\text{g-C}_3\text{N}_4$ reaches the value 2.7 eV, what predetermines the possibility of its activation with the light of wavelength 460 nm and lower and therefore its ability to use a significantly higher proportion of daylight for its activation. $\text{G-C}_3\text{N}_4$ is often synthesized via thermal polymerization of melamine at the temperatures in the range of 550 – 600 °C, and the so-called bulk- $\text{g-C}_3\text{N}_4$ is obtained. One of the parameters limiting the bulk- $\text{g-C}_3\text{N}_4$ photodegradation activity is its low specific surface area, which is often reported around $10 \text{ m}^2\cdot\text{g}^{-1}$. $\text{G-C}_3\text{N}_4$ has layered structure similar with graphite, and using the exfoliation, its surface area can be significantly increased, and the values in the range of 100 – 200 $\text{m}^2\cdot\text{g}^{-1}$ are reported. Increasing of specific surface area leads to significant increase in photodegradation activity of $\text{g-C}_3\text{N}_4$. Despite the excellent photocatalytic properties of $\text{g-C}_3\text{N}_4$, only a few reports on the possibilities of using $\text{g-C}_3\text{N}_4$ in the field of inorganic building materials have been published in recent years, for example, [8, 9].

In our research we tested the application of both bulk- C_3N_4 and exfoliated $\text{g-C}_3\text{N}_4$ on the surface of sand stones with the aim to reveal its ability to ensure the self-cleaning properties of such treated surface. The self-cleaning performance of the surfaces was tested using discoloration of rhodamine B applied on the sand-stone samples.

2. MATERIALS AND METHODS

2.1 Sample preparation

Bulk $\text{g-C}_3\text{N}_4$ was prepared by thermal polycondensation of melamine precursor. In a typical procedure, 10 grams of melamine was put to ceramic crucible, which was covered with a ceramic lid and calcined for 4h at 550 °C in a muffle furnace. After the calcination step, the sample was let to cool down slowly in a furnace. The resulting bulk $\text{g-C}_3\text{N}_4$ was labelled as Bulk-gCN.

Sandstone from the locality of Mšené-lázně (Czech Republic) was chosen for the experiment because of its light and relatively homogeneous colour.

Exfoliation of g-CN was performed thermally at 600 °C. In this process, approximately 0.5 g of bulk gCN was placed on the bottom of ceramic dish to form thin layer. Such prepared sample was heated at 600 °C for 45 min and the sample was labelled TEX45.

From TEX45 sample, the suspensions were prepared in demineralized water, with concentrations of $2\text{g}\cdot\text{dm}^{-3}$ and $4\text{g}\cdot\text{dm}^{-3}$. The suspensions were mixed in the Omni Sonic Ruptor 400 Ultrasonic Homogenizer, for 15 minutes. The prepared suspensions were applied to the surface of test specimens of sand stones by spraying, and samples TEX45/2 and TEX45/4 were obtained.

2.2 Sample characterization

Carbon, hydrogen and nitrogen content of prepared samples was determined on instrument LECO 828 (LECO, USA). Typically, around 100 mg of sample was loaded in tin foil, in a next step the tin foil with sample was gently squeezed and such prepared sample was loaded to an autosampler.

X-ray diffraction (XRD) analysis was performed using MiniFlex600 theta/2theta diffractometer (Rigaku, Japan) equipped with Co tube ($\lambda = 1,78897 \text{ \AA}$) and a 1D silicon strip D/teX Ultra250 detector. The powder sample was pressed in a rotational holder, the patterns were recorded in the range 10 – 80 °2Theta with step 0.02 °, and scan speed 3 °·min⁻¹. The obtained data were visualised using SW Origin 2020b.

Scanning Electron Microscope (SEM) eXPLORER (ASPEX, USA) was used to observe the morphology of bulk-gCN and TEX120 samples. Before the measurement the samples were coated with an Au/Pd film, and the SEM images were obtained using a backscattered electron (BSE) detector.

UV-VIS DRS spectra were registered using Shimadzu UV-2600 UV-VIS spectrometer equipped with integrating sphere 2600Plus (Shimadzu Ltd). Powder samples were placed inside a dedicated holder with quartz window and the spectra were recorded at room temperature in the range 200-800nm. Barium sulphate powder was used for base line registration. Tauc's plots [12] were used to evaluate indirect band gap energies.

Specific surface area of the samples was obtained with the method based on physisorption of nitrogen using an instrument Sorptomatic 1990 (Thermo Scientific, USA). The data of adsorbed volume of nitrogen was registered in the range of 0.05 – 0.25 of relative pressure. The obtained data were evaluated using Brunauer–Emmett–Teller (BET) method.

The photodegradation activity of the prepared samples was evaluated by photodegradation Rhodamine B (RhB). In a typical experiment 0.05 g of sample was weighted into 200 ml glass baker and 150 ml of RhB water solution ($10 \text{ mg} \cdot \text{dm}^{-3}$) was added. Such prepared suspension was subjected to irradiation with the light of wavelength 420 nm (FWHM 10 nm) under continuous stirring. In selected time intervals (0 and 120 min) 2ml of suspension was sampled using syringe and further filtered using syringe filter (CHROMAFIL GF/RC-20/25 filters, Macherey-Nagel, Germany) directly to 1 cm microcuvettes made of quartz glass. The absorbance of such collected filtrate was measured at 580 nm using UV-2600 spectrometer (Shimadzu, Japan). The obtained absorbance values at given irradiation time were recalculated to RhB concentration using the method of calibration curve.

The self-cleaning test was conducted using method derived from UNI 11259:2008 standard. This method is based on the discoloration of rhodamine B applied on the surface of tested samples. Our procedure included application of rhodamine B solution with concentration of $50 \text{ g} \cdot \text{dm}^{-3}$ on the sample surfaces using lab sprayer. After the RhB application, the samples were conditioned in a dark in climate chambre ICH110L (Mettler, Germany) for 24 h at a temperature of $20 \text{ }^\circ\text{C}$ and a relative humidity of 60 %. The climate chamber is equipped with an illumination source simulating a day light and after 24h dark period, the relative humidity inside the chambre was raised to 70%, and the illumination was started. The colorimetric coordinates $L^*a^*b^*$ of the samples were measured after 4 and 26h of irradiation. The relative changes in coordinate a^* at given time of irradiation in comparison with this value measured before the irradiation were calculated and expressed as R_4 and R_{26} .

Colorimetric measurements on the test specimens, with the aim to obtain the values of $L^*a^*b^*$ coordinates, were performed using MiniScan EZ 4500S spectrophotometer (HunterLab, VA, USA). The system uses xenon lamps, and intensity of the light reflection lies in the range of visible light spectrum ($\lambda = 400\text{--}700 \text{ nm}$).

3. RESULTS AND DISCUSSION

Carbon, nitrogen and hydrogen content was determined using elemental analysis, and the results are compared for both samples in **Table 1**.

Table 1 Specific surface area and band gap energy of the prepared samples

Samples	C (wt.%)	H (wt.%)	N (wt.%)	C/N	SSA ($\text{m}^2 \cdot \text{g}^{-1}$)	Eg (eV)
Bulk-gCN	33.6	1.81	59.6	0.56	10	2.67
TEX45	31.7	2.25	61.4	0.51	78	2.72

As evident in **Table 1**, the sum of these elemental contents does not reach 100 wt.% and for both samples, around 5 wt.% is missing and this content corresponds to oxygen, which was not determined. Carbon content decreased in the case of sample TEX45, while hydrogen and nitrogen contents increased in this sample. The C/N ratio calculated for Bulk-gCN reached the value 0.56 and indicates a non-fully polymerized gCN structure, which has this ratio 0.64. The decrease in C/N ratio observed for sample TEX45 (see **Table 1**) is in good

agreement with the results observed by the other authors [10], indicating that the carbon of the tri-s-triazine building blocks was attacked and burn out during the thermal exfoliation process.

The morphology of the bulk-gCN and TEX45 particles was observed with SEM and the micrographs obtained are compared in **Figure 1**. Bulk-gCN particles (**Figure 1a**) have a compact flaky character, while TEX45 particles (**Figure 1b**) exhibit a spongy character, with distinctive pores of large size. The formation of pores in TEX45 documented with SEM supports the results of the chemical composition (**Table 1**), when the decrease in the carbon content was observed for TEX45 and was explained by burning of the carbon of the tri-s-triazine building blocks.

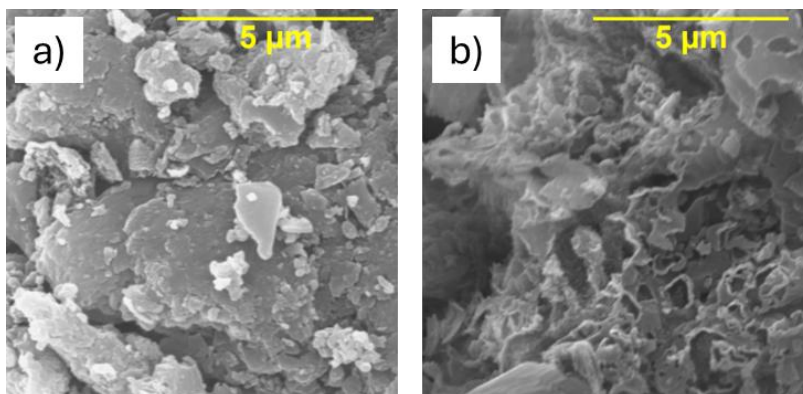


Figure 1 SEM micrographs of samples a) bulk-gCN, and b) TEX45

The structure of both samples was studied using the XRD method and the registered diffraction patterns are shown in **Figure 2a**). The strong diffraction peak centered at approximately $32^\circ 2\theta$ (CoK α) corresponds to the (002) plane and is characteristic for the interlayer stacking of aromatic systems, while the low intensity diffraction peak centered at around $15^\circ 2\theta$ (CoK α) belonging to the (100) planes corresponds to the interplanar separation [11]. The character of both diffraction patterns is closely similar and indicates that the character of g-C₃N₄ remained unchanged after exfoliation. A slight shift of the maxima of the TEX45 (002) diffraction peak towards higher angles is related to a denser packing of g-C₃N₄ layers.

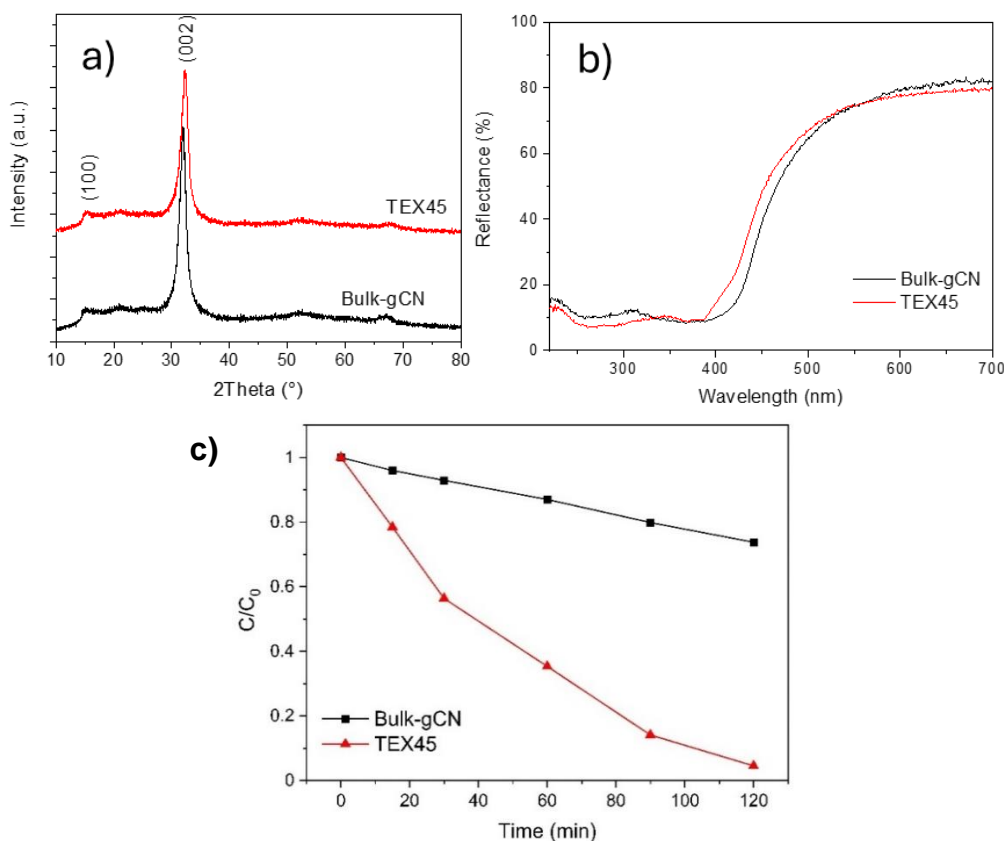
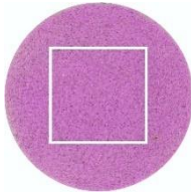
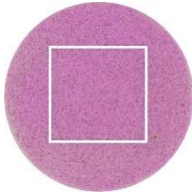
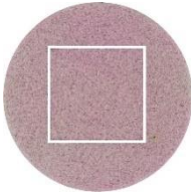
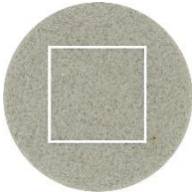
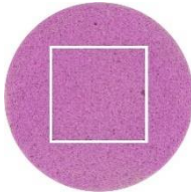
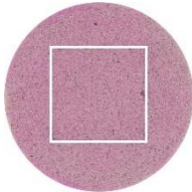
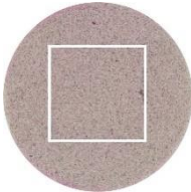


Figure 3 Comparison of photodegradation activity of tested samples bulk-gCN, and b) TEX45

Based on the photodegradation results, the TEX45 sample was used to coat of the surface of the sand stone samples and the results are summarized in **Table 2**. The pictures of the sand stone samples coloured with RhB show the progressive change in their colour appearance with irradiation time.

Table 2 Results of the self-cleaning test

Sample	R _x	Before test	After 4 h	After 26 h	Original colour
TEX45/2	R ₄ = 10.5 R ₂₆ = 59.6				
TEX45/4	R ₄ = 31.5 R ₂₆ = 72				

The calculated values of R₄ and R₂₆ clearly indicate that application of the TEX45 suspension of concentration of 4g·dm⁻³ (sample TEX45/4), showed significantly higher value R₂₆, and thus indicates higher self-cleaning performance of this sample.

4. CONCLUSION

The research proved that the application of exfoliated graphitic carbon nitride on the porous surface of sand stones imparted self-cleaning abilities to this important building material. The results proved a higher self-cleaning ability for the sand stone sample, whose surface was covered with a higher amount of TEX45. Sand stones are highly porous material and the solution of the RhB dye easily penetrates inside the pores. Next studies will focus on the search for the hydrophobic agent, which could easily be added to exfoliated gCN suspensions and which would block the penetration of the RhB solution to the pores of the sand stones.

ACKNOWLEDGEMENTS

This research was supported by the Czech Science Foundation (project 24-10949S), while the infrastructure has been utilized in the frame of project No. CZ.02.01.01/00/22_008/0004631 Materials and technologies for sustainable development within the Jan Amos Komensky Operational Program financed by the European Union and from the state budget of the Czech Republic. Authors also thank to project SP2024/025 (VSB – Technical University of Ostrava).

DATA AVAILABILITY

[10.5281/zenodo.13927505](https://doi.org/10.5281/zenodo.13927505)

REFERENCES

- [1] ZHAO, L., DENG, J., SUN, P., LIU, J., JI, Y., et al. Nanomaterials for treating emerging contaminants in water by adsorption and photocatalysis: Systematic review and bibliometric analysis. *Science of The Total Environment*. 2018, vol. 627, pp. 1253-1263.

- [2] BANG TRUONG, H., CUONG NGUYEN, X. and HUR, J. Recent advances in g-C₃N₄-based photocatalysis for water treatment: Magnetic and floating photocatalysts, and applications of machine-learning techniques. *Journal of Environmental Management*. 2023, vol. 345.
- [3] CHEN, X., QIAO, L., ZHAO, R., WU, J., GAO, J., et al. Recent advances in photocatalysis on cement-based materials. Online. *Journal of Environmental Chemical Engineering*. 2023, vol. 11, pp. 109416
- [4] KLIENCHEN DE MARIA, V.P., et al., Advances in ZnO nanoparticles in building material: Antimicrobial and photocatalytic applications – Systematic literature review. *Construction and Building Materials*. 2024, vol. 417. pp. 135337.
- [5] PAOLINI, R., et al., Self-cleaning building materials: The multifaceted effects of titanium dioxide. *Construction and Building Materials*. 2018, vol. 182, pp. 126-133.
- [6] ŽERJAV, G., et al., Brookite vs. rutile vs. anatase: What's behind their various photocatalytic activities? *Journal of Environmental Chemical Engineering*. 2022, vol. 10, pp. 107722
- [7] WANG, X., et al., A metal-free polymeric photocatalyst for hydrogen production from water under visible light. *Nature Materials*. 2009, vol. 8, pp. 76-80.
- [8] PENG, F., et al., New g-C₃N₄ based photocatalytic cement with enhanced visible-light photocatalytic activity by constructing muscovite sheet/SnO₂ structures. *Construction and Building Materials*. 2018, vol. 179, pp. 315-325.
- [9] YANG, Y., et al., Efficiency and durability of g-C₃N₄-based coatings applied on mortar under peeling and washing trials. *Construction and Building Materials*. 2020, vol. 234, pp. 117438.
- [10] Li, Y., et al., Tuning and thermal exfoliation graphene-like carbon nitride nanosheets for superior photocatalytic activity. *Ceramics International*. 2016, vol. 42, pp. 18521-18528.
- [11] CAO, S., et al., Polymeric Photocatalysts Based on Graphitic Carbon Nitride. *Advanced Materials*. 2015, vol. 27, pp. 2150-2176.